

Nanoscale Critical Phenomena in a Complex Fluid Studied by X-Ray Photon Correlation Spectroscopy

D. Sheyfer^{1,*} Qingteng Zhang² J. Lal,^{1,3} T. Loeffler,⁴ E. M. Dufresne² A. R. Sandy² S. Narayanan,²
S. K. R. S. Sankaranarayanan,^{4,5} R. Szczygiel⁶ P. Maj,⁶ L. Soderholm⁷ M. R. Antonio⁷ and G. B. Stephenson^{1,†}

¹Materials Science Division, Argonne National Laboratory, Argonne, Illinois 60439, USA

²X-Ray Science Division, Argonne National Laboratory, Argonne, Illinois 60439, USA


³Department of Physics, Northern Illinois University, DeKalb, Illinois 60115, USA

⁴Nanoscale Science and Technology Division, Argonne National Laboratory, Argonne, Illinois 60439, USA

⁵Department of Mechanical and Industrial Engineering, University of Illinois, Chicago, Illinois 60607, USA

⁶AGH University of Science and Technology, Krakow 30-059, Poland

⁷Chemical Science and Engineering Division, Argonne National Laboratory, Argonne, Illinois 60439, USA

 (Received 28 March 2020; revised 27 May 2020; accepted 14 July 2020; published 18 September 2020)

The advent of high-speed x-ray photon correlation spectroscopy now allows the study of critical phenomena in fluids to much smaller length scales and over a wider range of temperatures than is possible with dynamic light scattering. We present an x-ray photon correlation spectroscopy study of critical fluctuation dynamics in a complex fluid typical of those used in liquid-liquid extraction (LLE) of ions, dodecane-DMDBTDMA with extracted aqueous $\text{Ce}(\text{NO}_3)_3$. We observe good agreement with both static and dynamic scaling without the need for significant noncritical background corrections. Critical exponents agree with 3D Ising values, and the fluctuation dynamics are described by simple exponential relaxation. The form of the dynamic master curve deviates somewhat from the Kawasaki result, with a more abrupt transition between the critical and noncritical asymptotic behavior. The concepts of critical phenomena thus provide a quantitative framework for understanding the structure and dynamics of LLE systems and a path forward to new LLE processes.

DOI: [10.1103/PhysRevLett.125.125504](https://doi.org/10.1103/PhysRevLett.125.125504)

The nanoscale structure that develops near critical points is particularly fascinating in complex fluids [1,2], where it offers the opportunity to enhance behavior such as ion transport [3]. Concepts from the theory of critical phenomena [4,5] are a potentially powerful framework to understand these phenomena. As the critical point is approached, the divergences of correlation lengths, susceptibilities, and fluctuation timescales can be described by scaling laws with universal features for a given class of transition [6,7]. Studies of pure and binary small-molecule fluids have allowed detailed verification of predicted nonclassical exponents very close to the critical temperature T_c , with indications of crossover to classical exponents as $|T - T_c|$ is increased [8]. In contrast, studies of complex fluids containing micelles [9–12], microemulsions [13–16], or macromolecules [17] have typically found less complete agreement, often requiring large noncritical background corrections or other theoretical modifications [18,19].

One of the most powerful methods used to characterize critical fluctuations in fluids has been dynamic light scattering (DLS), in which time correlations in the speckle pattern produced by the scattering of a coherent light beam allow the observation of fluctuation dynamics [20]. However, DLS only reveals the behavior on length scales comparable to or larger than the wavelength of visible light.

This often restricts the study of critical phenomena to temperatures close to T_c , where the correlation length grows to this length scale [6,8,21]. Here we present a study using the x-ray analog of DLS, known as x-ray photon correlation spectroscopy (XPCS) [22,23]. The shorter x-ray wavelength provides the first opportunity to study the dynamics of critical fluctuations having much smaller length scales over a correspondingly larger temperature region around T_c . This allows us to investigate the extent to which both static and dynamic scaling laws apply to this larger region.

The system we study is a complex fluid typical of those used in liquid-liquid extraction (LLE), an energy-efficient separation option used for the purification of a variety of chemicals, including rare-earth elements [24,25]. Figure 1 shows the schematic phase diagram of this system [26]. It consists of a small-molecule organic solvent, dodecane, mixed with a large-molecule amphiphilic extractant, N,N'-dimethyl-N,N'-dibutyltetradecylmalonamide (DMDBTDMA), which facilitates the dissolution of polar ions into the nonpolar phase through the formation of nanoscale molecular complexes resembling small reverse micelles [27,28]. Here, aqueous ions are extracted from an acidic $\text{Ce}(\text{NO}_3)_3$ solution. After equilibration with the aqueous phase, we isolate the organic phase containing

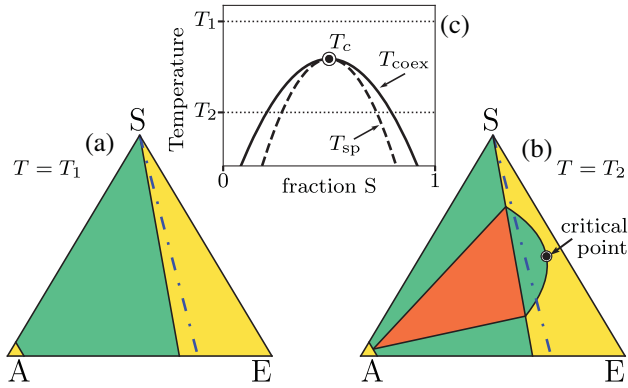


FIG. 1. Schematic phase diagram for a liquid-liquid extraction system, expressed as a ternary system between aqueous solution A, organic solvent S, and amphiphilic extractant E. (a),(b) Isothermal cuts above and below, respectively, the temperature at which the 3-phase region and associated critical point appear. Colors denote 1-phase regions (yellow), 2-phase regions (green), and 3-phase regions (orange). (c) Pseudobinary cut at fixed A/E ratio given by dash-dot line in (a),(b), showing the coexistence (solid) and spinodal (dashed) curves.

extracted polar ions. Upon cooling, it separates into high- and low-extractant organic phases at T_{coex} , as shown in Fig. 1(c). At the critical composition, this corresponds to T_c ; away from this composition, the instability occurs below T_{coex} at the spinodal temperature T_{sp} [16,29]. Efficient chemical separation using LLE is often carried out near, but not too close to, this instability where the correlation length of the complexes becomes large but organic phase splitting is avoided [30]. Understanding the critical behavior of the nanoscale complexes is thus of great practical interest [31]. A goal of this study is to test the applicability of the concepts of static and dynamic critical phenomena to this important class of complex fluids.

Our XPCS measurements of critical fluctuation dynamics in fluids were made possible not only by the advent of coherent x-ray methods at high-brightness synchrotron sources, but also by the recent development of high-speed x-ray area detector systems [32] that can reach the microsecond time regime typical for fluid fluctuations. This fills in a capability gap between previous slower XPCS studies and alternative methods to observe equilibrium nanoscale dynamics that are sensitive only to much shorter timescales, such as inelastic neutron and x-ray scattering [22,23,33]. The new pixel-array detector used had 32768 pixels that could be read with a 50 kHz frame rate to allow multispeckle XPCS with a 20 microsecond time resolution. The only previous XPCS study of critical fluctuation dynamics in a fluid [34] used a single-pixel detector to achieve the needed time resolution, which limited the range of conditions that could be investigated.

The XPCS experiments were conducted at beamline 8-ID-I of the Advanced Photon Source. The x-ray energy of 10.9 keV and angular range of 0.4 to 2.7 mrad gave access

to a wave number q range of 0.0024 to 0.0152 \AA^{-1} . Details of the sample preparation, experimental setup, and data reduction can be found in the Supplemental Material [35]. The sample had a ratio of extractant to solvent close to the critical value. Data were collected at a set of fixed temperatures approaching T_{coex} from above by cooling from an initial T of 298.2 K.

We first analyzed the time-averaged scattering at each T using the scaling laws for static critical phenomena. Figure 2 shows the normalized and background-subtracted scattered intensity as a function of q at selected temperatures. For the initial temperature steps well above T_{sp} , a decrease in T increases the scattered intensity at all measured q . As T_{sp} is approached, the scattered intensity saturates at higher q , while it continues to increase at lower q . The saturated intensities reach an asymptote that is well described by a power-law dependence on q . Such behavior, previously observed in similar LLE systems [30,49], is consistent with an increasing correlation length ξ of thermal fluctuations near T_{sp} and the formation of a scale-invariant structure. The maximum intensity is reached at 291.6 K; further cooling produces a decrease in intensity at all q consistent with separation into two phases with low- and high-extractant concentrations at $T_{\text{coex}} = 291.5 \pm 0.1$ K [Fig. 1(c)].

The scattering data at a given temperature above T_{sp} can be described by [50]

$$I(q, T) = I_{q_0}(T)/(1 + x^{2-\eta}), \quad (1)$$

where the reduced wave number x is defined by $x \equiv q\xi(T)$. Here the ‘‘dimensional anomaly’’ [4] exponent η can deviate from the classical Ornstein-Zernike value of $\eta = 0$. Data for all 20 temperatures were simultaneously fit using Eq. (1) with 41 parameters: I_{q_0} and ξ for each T , and a single value of η . The values of I_{q_0} and ξ obtained are shown in Fig. 2(b), (c). Data for all temperatures rescaled using these values collapse onto a single master curve, as shown in the inset to Fig. 2(a). The best-fit exponent is $\eta = 0.064 \pm 0.001$.

The susceptibility I_{q_0} and correlation length ξ are expected to diverge at T_{sp} following the expressions [4]

$$I_{q_0}(T) = I_0[(T - T_{\text{sp}})/T_{\text{sp}}]^{-\gamma}, \quad (2)$$

$$\xi(T) = \xi_0[(T - T_{\text{sp}})/T_{\text{sp}}]^{-\nu}. \quad (3)$$

Fits to obtain the critical exponents γ and ν , the amplitudes I_0 and ξ_0 , and the spinodal temperature T_{sp} are shown in Fig. 2(b),(c). The two fits give the same value $T_{\text{sp}} = 291.3 \pm 0.1$ K. The obtained values of the critical exponents, $\gamma = 1.24 \pm 0.06$ and $\nu = 0.64 \pm 0.03$, agree with the accepted values for the 3D Ising model, $\gamma = 1.23$ and $\nu = 0.63$ [8]. In addition, the exponents obey the relation $\gamma = (2 - \eta)\nu$ [4], as indicated by the intensity curves at all T approaching a common asymptote at $x \gg 1$. The small

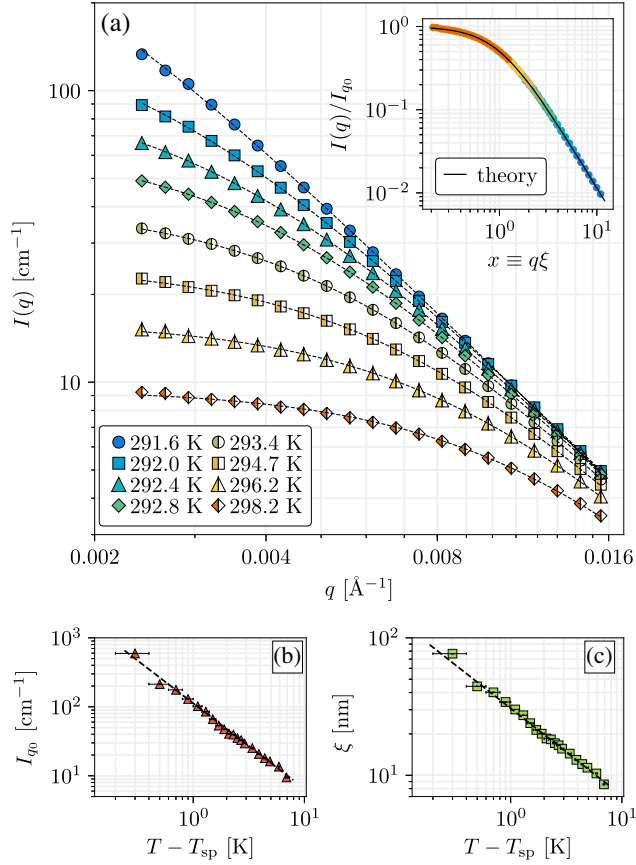


FIG. 2. Time-averaged results. (a) Normalized scattered intensity I as a function of wave number q for different temperatures, plotted on logarithmic scales. Only selected values of the total 20 T and 180 q values measured are shown. Curves are fits with Eq. (1). Inset: Data at all temperatures rescaled using parameters obtained from fits. (b),(c) Plots of fit parameters I_{q0} and ξ vs $T - T_{sp}$, showing power-law fits. Values with uncertainties are given in the Supplemental Material [35], Table S1.

difference $T_{\text{coex}} - T_{\text{sp}} = 0.2$ K indicates that the sample is close to the critical composition.

The fluctuation dynamics can be characterized by the intensity autocorrelation function $g^{(2)} = \langle I(q, t)I(q, t + \Delta t) \rangle / \langle I(q, t) \rangle^2$ measured by XPCS [22,23]. While the signal levels in each 20 microsecond exposure were quite low, e.g., 10^{-3} photons per pixel, it was possible to obtain acceptable signal to noise in $g^{(2)}$ for the 18 temperatures closest to T_{sp} and q values out to 0.0065 \AA^{-1} by averaging over pixels within narrow bands of q and over hundreds of repeats of acquisition sequences, each a few seconds long [35]. Typical observed $g^{(2)}(\Delta t)$ are shown in Fig. 3(a) at $T = 291.6$ K and various q . As expected, the $g^{(2)}$ function decays faster at larger q , indicating faster fluctuation dynamics at smaller length scales. The form of $g^{(2)}(\Delta t)$ is well described by a single exponential decay, with a relaxation time τ obtained by fitting to [23]

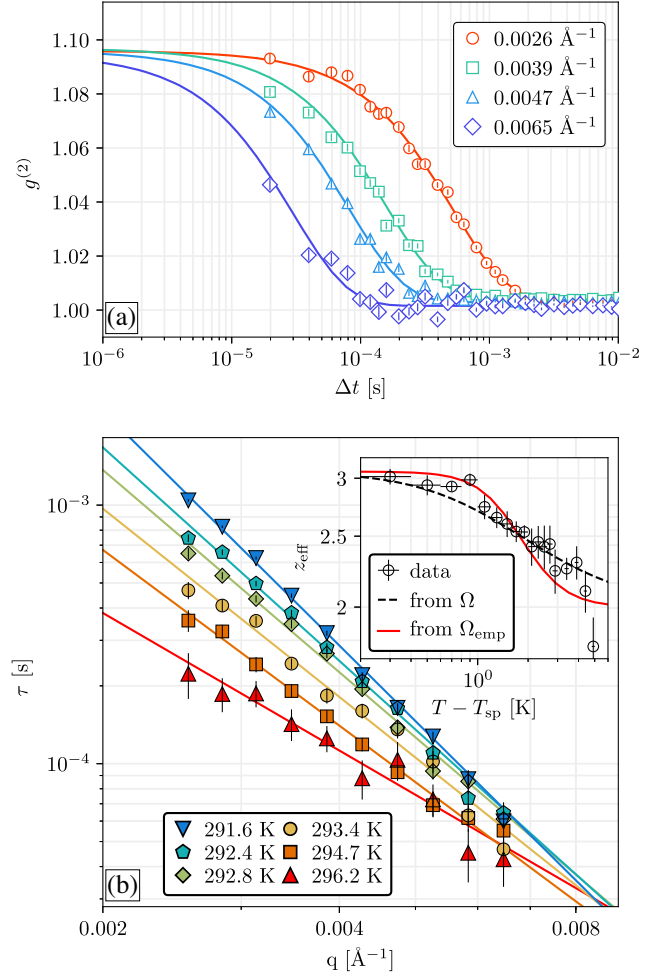


FIG. 3. Dynamics of LLE system. (a) Measured $g^{(2)}(\Delta t)$ at $T = 291.6$ K and selected q , showing fits (curves) using Eq. (4). (b) Extracted fluctuation correlation times τ as a function of q at selected T , showing fits (lines) to obtain power-law slopes $-z_{\text{eff}}$. Inset: Effective dynamic critical exponent z_{eff} as a function of T for the q range of the measurements.

$$g^{(2)} = B + \beta \exp(-2\Delta t/\tau), \quad (4)$$

where β is a constant contrast parameter related to the coherence properties of the x-ray beam and the scattering geometry, and B is a baseline parameter close to unity. For our setup, the contrast was determined to be $\beta = 0.093$, and only τ and B were varied in the fits [35]. Typical fits are shown with the data in Fig. 3(a). Figure 3(b) shows the dependence of the relaxation time τ on q for different T . At each temperature, the q dependence of τ is reasonably well described by a simple power law over the q range for which τ can be extracted. As T_{sp} is approached, the τ values at lower q increase more rapidly than those at higher q , giving a change in the power-law exponent. Power-law fits to $\tau \propto q^{-z_{\text{eff}}}$ at each T are shown with the data in Fig. 3(b), and the obtained values of the effective dynamic critical exponent z_{eff} are shown in the inset.

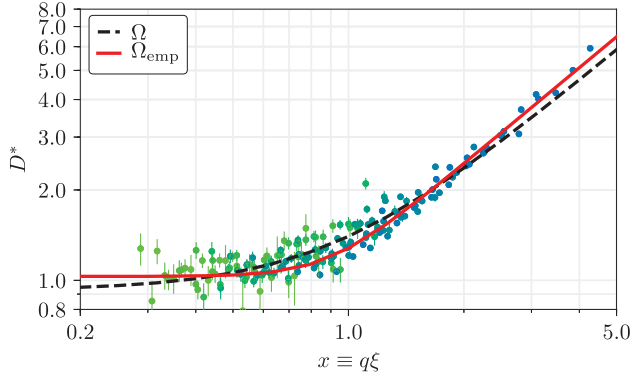


FIG. 4. Reduced diffusivity D^* vs reduced wave number $x \equiv q\xi$ for all q and T , compared to modified Kawasaki scaling function Ω and empirical function Ω_{emp} . Color of markers indicates T of experimental data points: green (296.2 K) to blue (291.6 K). Residuals of the two fits are compared in [35].

The full dependence of the fluctuation relaxation time on q and T near T_{sp} has been described by dynamic scaling theory [51–54]. This is typically given in terms of the wave number-dependent diffusivity related to τ by $D \equiv 1/(\tau q^2)$, which can be written as

$$D(q, T) = D_0(T)\Omega(x) + \bar{D}(q, T). \quad (5)$$

Here $D_0 = k_B T / (6\pi\eta_s \xi)$ is an estimate [51–53] of the q -independent value well away from T_{sp} , where η_s is the shear viscosity, and \bar{D} is a noncritical background correction [54]. In our case, the contribution of this term is small, less than a few percent [35]. The wave-number dependence for any T enters primarily through the scaling function $\Omega(x)$ of the reduced wave number x . Mode-coupling theory [54] gives the form of $\Omega(x)$ as

$$\Omega(x) = R\Omega_K(x)(1 + b^2 x^2)^{z_\eta/2}, \quad (6)$$

where R is a constant with a value near unity, Ω_K is the Kawasaki scaling form [51]

$$\Omega_K(x) = (3/4)x^{-2}[1 + x^2 + (x^3 - x^{-1}) \arctan(x)], \quad (7)$$

and the final factor in Eq. (6) has parameters $b \approx 0.55$ and $z_\eta \approx 0.063$ [54].

Figure 4 shows the rescaled experimental relaxation times for all T plotted as reduced diffusivity $D^* \equiv (D - \bar{D})/D_0$ vs x , using measured values of the viscosity [35]. Also shown is the theory expression for $\Omega(x)$ from Eq. (6), fit to the experimental D^* using a single free parameter R . This fit gives a value $R = 0.90 \pm 0.01$.

The power-law slope of $\tau(q)$ can be obtained from Eq. (6) as

$$z_{\text{eff}}(q, T) \equiv -\left. \frac{\partial \ln \tau}{\partial \ln q} \right|_{q, T} \approx 2 + \left. \frac{\partial \ln \Omega(x)}{\partial \ln x} \right|_{x=q\xi(T)}, \quad (8)$$

where the small term in Eq. (5) has been neglected. This theoretical curve is plotted along with the experimental values in the inset of Fig. 3(b) using the average value of $q = 0.004 \text{ \AA}^{-1}$ to extract the experimental z_{eff} .

The use of x-ray scattering allows a direct determination of the correlation length ξ , its scaling exponents η and ν , and relaxation times τ out to relatively high q . This increases the window of $T - T_{\text{sp}}$ that can be studied and provides a broader comparison with critical phenomena predictions. Our results show remarkably good agreement with both static and dynamic scaling predictions for binary fluids across a wide range of q and $T - T_{\text{sp}}$. All $I(q, T)$ collapse onto a single static master curve [see the Fig. 2(a) inset] with power-law behavior of scaling parameters I_{q0} and ξ as a function of $T - T_{\text{sp}}$. The values of the exponents ν , γ , and η agree with those for the 3D Ising model and verify the relation $\gamma = (2 - \eta)\nu$. Likewise, we observe good general agreement with dynamic scaling. We observe a single exponential relaxation time at each q and T . All $D^*(q, T)$ collapse onto a single master curve using the same scaling parameter ξ and the standard form for D_0 , as shown in Fig. 4. The asymptotes of the master curve agree with the predicted behavior, giving a change in z_{eff} from 2 to $3 + z_\eta$ as T_{sp} is approached. However, the detailed shape of the master curve appears to deviate from that given by the modified Kawasaki form Ω , with the transition between the asymptotic behavior above and below $x = 1$ more abrupt than predicted. This can also be seen in the T dependence of z_{eff} in the Fig. 3(b) inset.

To quantify this deviation, we fit the dynamic master curve to an empirical form that obeys the asymptotes of $\Omega(x)$ at $x \ll 1$ and $x \gg 1$,

$$\Omega_{\text{emp}} = R\{1 + [(3\pi/8)b^{z_\eta} x^{1+z_\eta}]^m\}^{1/m}, \quad (9)$$

where m is a crossover exponent. While a fit of Eq. (9) to $\Omega(x)$ gives a value $m = 1.98$, a fit to the data gives $m = 4.8 \pm 0.5$ and $R = 1.03 \pm 0.01$. The fit of Eq. (9) to the data gives a reduced chi square of $\chi_r^2 = 2.5$ compared to $\chi_r^2 = 4.2$ from the fit of Eq. (6) to the data.

The 3D Ising model is expected to apply to systems with a scalar order parameter, such as the single compositional variable in a two-component fluid mixture. While in the ternary phase diagrams Fig. 1(a), (b) we have grouped the ions into the aqueous component, our system actually consists of five chemical components (dodecane, DMBTDMA, water, cations, anions). It has been predicted that the exponents in a ternary system can be renormalized relative to the 3D Ising values according to $\gamma^* = \gamma/(1 - \alpha)$, $\nu^* = \nu/(1 - \alpha)$, where $\alpha \approx 0.11$ is the specific heat critical exponent [55,56]. The agreement of our observed exponents

with the 3D Ising values without such renormalization indicates that it is a good approximation to treat the system as a pseudobinary [see Fig. 1(c)] and that fluctuations in other compositional dimensions are negligible.

The generally good agreement we find with 3D Ising model predictions differs from the results of several studies of other complex fluids. In other systems containing micelles [9–12], microemulsions [13–16], or macromolecules [17], large noncritical background corrections or other modifications to theory [18,19] were required to describe DLS measurements. In contrast, the typical LLE system we study is well described by the standard static and dynamic critical behavior found for small-molecule binary fluids [8,54] and some micellar systems [57]. Thus, the detailed predictions of critical phenomena theory can provide a quantitative understanding to model the structure and dynamics of LLE systems.

The ability to carry out high-speed XPCS opens a new window into studies of fluctuation dynamics in fluids. XPCS studies were previously limited to high viscosity liquids or relatively large colloidal particles at low q . High-speed XPCS gives access to the faster timescales characteristic of higher q and thus allows greater exploration of the critical region $q\xi > 1$. The orders-of-magnitude increase in coherent x-ray flux soon to become available at upgraded facilities [58] will further expand the range of q and $T - T_c$, along with the fluid systems that can be explored.

We acknowledge the expert technical assistance of R. Ziegler. Studies of critical phenomena in LLE systems were supported by LDRD funding from Argonne National Laboratory, provided by the Office of Science (OS) of the U.S. Department of Energy (DOE) under Contract No. DE-AC02-06CH11357. Use of the APS, a DOE OS User Facility operated by Argonne, was supported under the same contract. We acknowledge support from DOE OS, Office of Basic Energy Sciences, Materials Science and Engineering division (XPCS method and analysis development) and Chemical Sciences, Geosciences, and Biosciences division (separation science). The detector development was supported by the National Centre for Research and Development, Poland (PBS1/A3/12/2012) and by NAWA - Polish National Agency for Academic Exchange, under Contract No. PPI/APM/2018/1/00049/U/001.

*Corresponding author.
dsheyfer@anl.gov

†Corresponding author.
gbs@anl.gov

- [1] M. Bier, J. Mars, H. Li, and M. Mezger, *Phys. Rev. E* **96**, 022603 (2017).
- [2] R. Motokawa, T. Kobayashi, H. Endo, J. Mu, C. D. Williams, A. J. Masters, M. R. Antonio, W. T. Heller, and M. Nagao, *ACS Cent. Sci.* **5**, 85 (2019).
- [3] R. Hayes, G. G. Warr, and R. Atkin, *Chem. Rev.* **115**, 6357 (2015).
- [4] M. E. Fisher, *Rev. Mod. Phys.* **70**, 653 (1998).
- [5] H. E. Stanley, *Rev. Mod. Phys.* **71**, S358 (1999).
- [6] A. L. Sengers, R. Hocken, and J. V. Sengers, *Phys. Today* **30**, No. 12 42 (1977).
- [7] P. C. Hohenberg and B. I. Halperin, *Rev. Mod. Phys.* **49**, 435 (1977).
- [8] J. V. Sengers and J. G. Shanks, *J. Stat. Phys.* **137**, 857 (2009).
- [9] J. Rouch, P. Tartaglia, A. Safouane, and S. H. Chen, *Phys. Rev. A* **40**, 2013 (1989).
- [10] D. Lombardo, F. Mallamace, N. Micali, and G. D'Arrigo, *Phys. Rev. E* **49**, 1430 (1994).
- [11] A. Martín, F. Ortega, and R. G. Rubio, *Phys. Rev. E* **54**, 5302 (1996).
- [12] J. Haller, R. Behrends, and U. Kaatz, *J. Chem. Phys.* **124**, 124910 (2006).
- [13] J. Rouch, A. Safouane, P. Tartaglia, and S. Chen, *J. Chem. Phys.* **90**, 3756 (1989).
- [14] J. Rouch, P. Tartaglia, and S. H. Chen, *Phys. Rev. Lett.* **71**, 1947 (1993).
- [15] S. H. Chen, J. Rouch, F. Sciortino, and P. Tartaglia, *J. Phys. Condens. Matter* **6**, 10855 (1994).
- [16] H. Seto, D. Schwahn, M. Nagao, E. Yokoi, S. Komura, M. Imai, and K. Mortensen, *Phys. Rev. E* **54**, 629 (1996).
- [17] B. M. Fine, J. Pande, A. Lomakin, O. O. Ogun, and G. B. Benedek, *Phys. Rev. Lett.* **74**, 198 (1995).
- [18] S. Chen, J. Rouch, and P. Tartaglia, *Physica (Amsterdam)* **204A**, 134 (1994).
- [19] K. Hamano, E. Ducros, E. Louisor, J. Rouch, and P. Tartaglia, *Physica (Amsterdam)* **231A**, 144 (1996).
- [20] B. J. Berne and R. Pecora, *Dynamic Light Scattering: With Applications to Chemistry, Biology, and Physics* (Wiley, New York, 1976).
- [21] H. C. Burstyn and J. V. Sengers, *Phys. Rev. A* **25**, 448 (1982).
- [22] O. G. Shpyrko, *J. Synchrotron Radiat.* **21**, 1057 (2014).
- [23] A. R. Sandy, Q. Zhang, and L. B. Lurio, *Annu. Rev. Mater. Res.* **48**, 167 (2018).
- [24] D. S. Sholl and R. P. Lively, *Nature (London)* **532**, 435 (2016).
- [25] A research agenda for transforming separation science, Technical Report, National Academy of Sciences, Washington, DC, USA, 2019.
- [26] C. Bauer, P. Bauduin, J. Dufrière, T. Zemb, and O. Diat, *Eur. Phys. J. Special Topics* **213**, 225 (2012).
- [27] F. Testard, T. Zemb, P. Bauduin, and L. Berthon, in *Ion Exchange and Solvent Extraction: A Series of Advances*, edited by B. A. Moyer (CRC Press, Boca Raton, 2010), Vol. 19, p. 381.
- [28] A. Karmakar, M. Duvail, M. Bley, T. Zemb, and J. Dufrière, *Colloids Surf. A* **555**, 713 (2018).
- [29] A. Wakker, J. F. van Baar, and W. J. van Lith, *Chem. Phys. Lett.* **174**, 263 (1990).
- [30] R. J. Ellis and M. R. Antonio, *Langmuir* **28**, 5987 (2012).
- [31] A. Clark, *ACS Cent. Sci.* **5**, 10 (2019).
- [32] Q. Zhang, E. M. Dufresne, S. Narayanan, P. Maj, A. Koziol, R. Szczygiel, P. Grybos, M. Sutton, and A. R. Sandy, *J. Synchrotron Radiat.* **25**, 1408 (2018).
- [33] R. Leheny, *Curr. Opin. Colloid Interface Sci.* **17**, 3 (2012).

- [34] E. M. Dufresne, T. Nurushev, R. Clarke, and S. B. Dierker, *Phys. Rev. E* **65**, 061507 (2002).
- [35] See Supplemental Material, which includes Refs. [36–48], at <http://link.aps.org/supplemental/10.1103/PhysRevLett.125.125504> for details on the sample preparation, methods, and analysis of static and XPCS data.
- [36] L. Berthon, L. Martinet, F. Testard, C. Madic, and T. Zemb, *Solvent extraction and ion exchange* **25**, 545 (2007).
- [37] C. Déjugnat, S. Dourdain, V. Dubois, L. Berthon, S. Pellet-Rostaing, J. Dufrêche, and T. Zemb, *Phys. Chem. Chem. Phys.* **16**, 7339 (2014).
- [38] T. Zemb, C. Bauer, P. Bauduin, L. Belloni, C. Déjugnat, O. Diat, V. Dubois, J. F. Dufrêche, S. Dourdain, M. Duvail, C. Larpent, F. Testard, and S. Pellet-Rostaing, *Colloid Polym. Sci.* **293**, 1 (2015).
- [39] R. J. Ellis, L. D’Amico, R. Chiarizia, and M. R. Antonio, *Sep. Sci. Technol.* **47**, 2007 (2012).
- [40] C. Erlinger, L. Belloni, T. Zemb, and C. Madic, *Langmuir* **15**, 2290 (1999).
- [41] F. Testard, P. Bauduin, L. Martinet, B. Abecassis, L. Berthon, C. Madic, and T. Zemb, *Radiochim. Acta* **96**, 265 (2008).
- [42] Y. Bard, *Nonlinear Parameter Estimation* (Academic Press, New York and London, 1974).
- [43] N. Draper and H. Smith, *Applied Regression Analysis* (John Wiley & Sons, New York, 1998).
- [44] K. Schatzel, *Quant. Opt.* **2**, 287 (1990).
- [45] F. Khan, S. Narayanan, R. Sersted, N. Schwarz, and A. Sandy, *J. Synchrotron Radiat.* **25**, 1135 (2018).
- [46] D. Abernathy, G. Grübel, S. Brauer, I. McNulty, G. Stephenson, S. Mochrie, A. Sandy, N. Mulders, and M. Sutton, *J. Synchrotron Radiat.* **5**, 37 (1998).
- [47] J. Verwohlt, M. Reiser, L. Randolph, A. Matic, L. A. Medina, A. Madsen, M. Sprung, A. Zozulya, and C. Gutt, *Phys. Rev. Lett.* **120**, 168001 (2018).
- [48] P. Vodnala, N. Karunaratne, L. Lurio, G. M. Thurston, M. Vega, E. Gaillard, S. Narayanan, A. Sandy, Q. Zhang, E. M. Dufresne, and G. Foffi, *Phys. Rev. E* **97**, 020601(R) (2018).
- [49] R. J. Ellis, *J. Phys. Chem. B* **118**, 315 (2014).
- [50] H. E. Stanley, *Introduction to Phase Transitions and Critical Phenomena* (Oxford University Press, New York, 1971).
- [51] K. Kawasaki, *Ann. Phys. (N.Y.)* **61**, 1 (1970).
- [52] R. A. Ferrell, *Phys. Rev. Lett.* **24**, 1169 (1970).
- [53] H. L. Swinney and D. L. Henry, *Phys. Rev. A* **8**, 2586 (1973).
- [54] H. C. Burstyn, J. V. Sengers, J. K. Bhattacharjee, and R. A. Ferrell, *Phys. Rev. A* **28**, 1567 (1983).
- [55] J. Rouch, A. Safouane, P. Tartaglia, and S. H. Chen, *Phys. Rev. A* **37**, 4995 (1988).
- [56] I. Iwanowski, S. Mirzaev, and U. Kaatz, *J. Chem. Phys.* **129**, 064516 (2008).
- [57] G. Dietler and D. S. Cannell, *Phys. Rev. Lett.* **60**, 1852 (1988).
- [58] R. Hettel, *J. Synchrotron Radiat.* **21**, 843 (2014).